# ALLUVIAL AND ELUVIAL PLATINUM-GROUP MINERALS FROM THE BUSHVELD COMPLEX, SOUTH AFRICA

T. OBERTHÜR
Bundesanstalt für Geowissenschaften und Rohstoffe (BGR), Stilleweg 2, D-30655 Hannover, Germany
e-mail: thomas.oberthuer@bgr.de

T.W. WEISER
Rischkamp 63, D-30659 Hannover, Germany.
e-mail: weiser@wandix.de

F. MELCHER
Institute of Geology and Economic Geology, University of Leoben, Peter-Tunnerstraße 5,
A-8700 Leoben, Austria.
e-mail: frank.melcher@unileoben.ac.at

© 2014 December Geological Society of South Africa

**ABSTRACT**

The present work provides an initial description of detrital platinum-group minerals (PGM) collected from alluvial sediments of rivers draining the Bushveld Complex, and from eluvial concentrations at the Onverwacht platiniferous pipe. During a field campaign, sediments were sampled at nine localities around the Bushveld Complex, and heavy mineral assemblages were investigated using optical and scanning electron microscopy (SEM) as well as microprobe analysis (EPMA) of PGM. All concentrates from the alluvial samples contain discrete PGM grains with grain sizes in the range from ~50 to 150 µm (maximum 600 µm). The overall PGM proportions are: native Pt, Pt-Pd and Pt-Fe alloys (together 54%), sperrylite (33%), cooperite/braggite (11%), and stibiopalladinite (2%). This PGM assemblage distinctly contrasts to the suite of PGM in the pristine, sulfide-bearing mineralization in the Merensky, UG-2 and Platreef, the assumed sources of the detrital PGM. Specifically, PGE-bismuthotellurides and -sulfarsenides, common in the primary ores, are missing in the assemblage of detrital PGM in the fluvial environment. Nearly all detrital PGM (98%) are Pt minerals, corroborating earlier findings that Pd-dominated PGM are unstable and are dissolved in the supergene environment, and that PGE-bismuthotellurides and -sulfarsenides, common in the PGM assemblages of the pristine ores are unstable during weathering and mechanical transport.

The eluvial material collected at Onverwacht contained ca. 150 PGM grains with sizes mainly in the range 100 to 300 µm range (maximum 1.87 mm). The PGM assemblage comprises grains of Pt-Fe alloys (66%), sperrylite (14%), and many rarer PGM including stibiopalladinite, hollingworthite, laurite, PGE arsenides and PGE sulfides. The suite of eluvial PGM observed is similar to the PGM assemblage described previously from the Onverwacht pipe proper, including the type locality minerals genkinite, irarsite and platarsite, as well as some additional and possibly new PGM. Most of the relatively rare PGM detected in the suite of eluvial grains from Onverwacht were also reported in the detrital PGM assemblage from the Moopetsi river, farm Maandagshoek (Oberthür et al., 2004), indicating that many of the latter grains originate from platiniferous pipes and not from the Merensky or UG-2 reefs.

Detrital PGM can be expected to be present in rivers draining PGE-bearing layered intrusions, and economic placers may form under particular sedimentological conditions. Therefore, this work also highlights the fact that the nowadays somewhat neglected field methods and basic techniques have their merits and value in mineral exploration, especially if they are combined with modern micro-analytical methods. The systematic recovery of PGM from stream sediments, soils and till should regain wider application in mineral exploration as these tools can provide useful indicators of platinum mineralization.

## Introduction

Placers in Colombia and in Russia (Ural mountains) were the major source of platinum-group minerals (PGM) before the discovery of the platinum deposits of the Bushveld Complex in South Africa. The initial major discovery of platinum in the Bushveld Complex, which subsequently led to the discovery of the Merensky Reef, was made in 1924 by panning in a river bed on the farm Maandagshoek in the Eastern Bushveld (Merensky, 1924; 1926; Wagner, 1929; Cawthorn, 1999, Oberthür et al., 2004). Wagner (1929) also reports on a number of alluvial diggings in the Bushveld Complex that produced some platinum. However, as mining commenced on the rich pipes and reef-type deposits of the Bushveld, alluvial PGM soon became forgotten because prospecting work in the 1920's did not reveal any placer occurrences of economic significance (Wagner, 1929). Therefore, only limited published information on placer PGM assemblages from the Bushveld rivers is available.

Our working group investigated the placer occurrences around the Merensky Reef discovery site on the farm Maandagshoek in the eastern Bushveld (Oberthür et al., 2004; Melcher et al., 2005), and the positive results of this undertaking prompted an

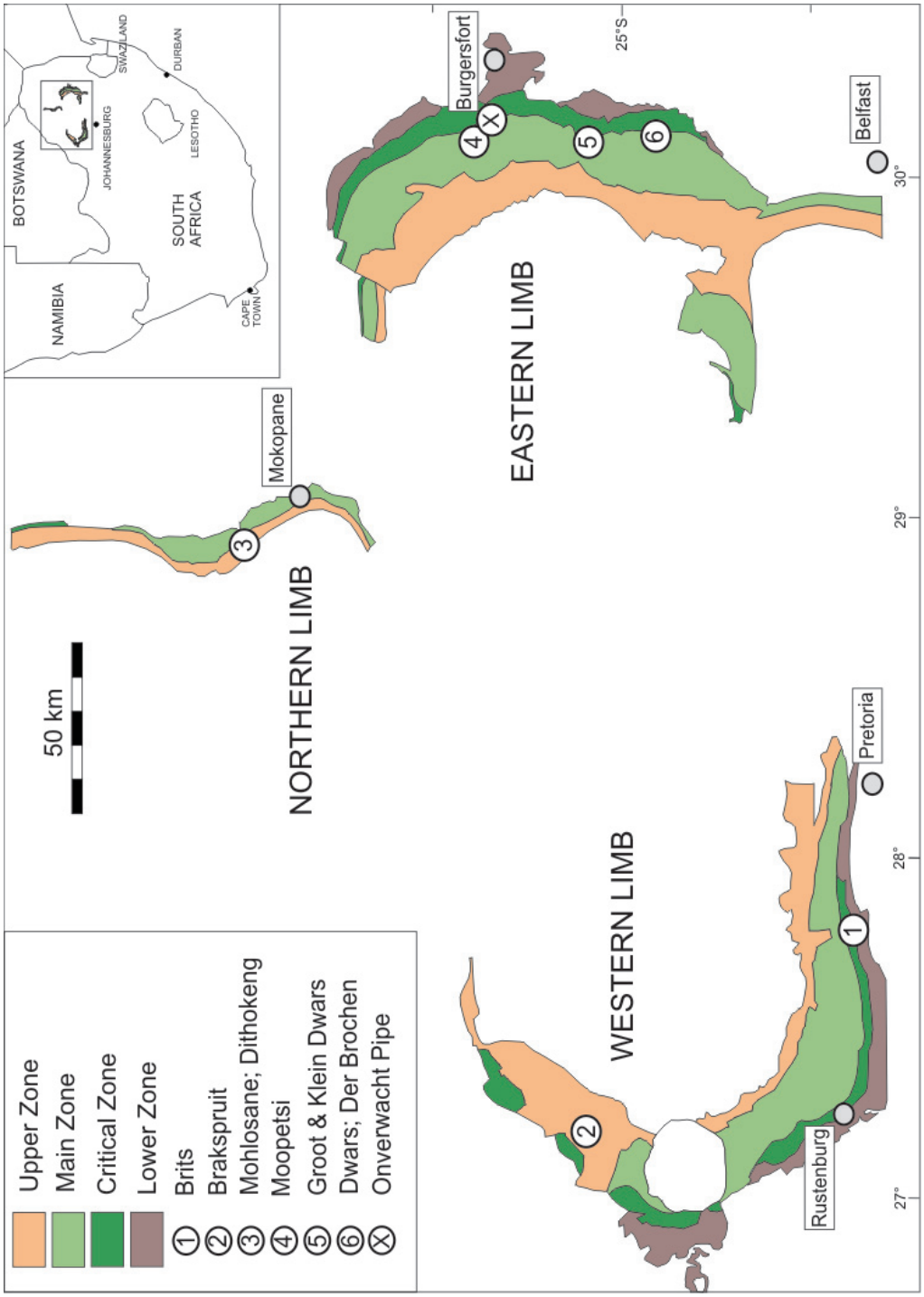


***Figure 1.*** *Generalized geology of the Bushveld Complex showing the stream sampling localities described in this study (1 to 6), and location of the Onverwacht Pipe (X).*

extended study of the alluvial sediments in rivers draining the whole Bushveld Complex, including the eluvial concentrations at the Onverwacht platiniferous pipe described by Wagner (1929).

**Previous work**

Knowledge of eluvial PGM in rivers on the Bushveld Complex is limited to the early compilation by Wagner (1929) which mainly concentrated on occurrences in the eastern Bushveld Complex. At that time, little information was available on the mineralogy of the PGM. Wilhelm et al. (1997) detected one detrital Pt-Fe alloy grain intergrown with laurite in their geochemical exploration campaign in the western Bushveld (Karee Spruit close to Brits). Oberthür et al. (2004) and Melcher et al. (2005) studied the placer accumulations on the farm Maandagshoek in the eastern Bushveld and identified a complex PGM assemblage originating from multiple sources (Merensky Reef, UG-2, and platiniferous pipes). Although the various platiniferous dunitic pipes of the eastern Bushveld are type localities of a number of PGM, systematic mineralogical examination of the ores is missing. The most information available is on the Driekop pipe (Stumpfl and Clark, 1965; Stumpfl, 1974; Tarkian and Stumpfl, 1975; Melcher and Lodziak, 2007). Work mainly on individual samples from the Onverwacht pipe was performed by Genkin et al. (1966), Cabri et al. (1977a; b; c), Rudashevsky et al. (1992), and Zaccarini et al. (2002). Genkin et al. (1966) and Cabri et al. (1977b; c) provided the first descriptions of the PGE minerals irarsite [IrAsS], genkinite [$(Pt,Pd)_4Sb_3$] and platarsite [PtAsS] from the Onverwacht type locality, whereas Rudashevsky et al. (1992) and Zaccarini et al. (2002) concentrated on the PGM assemblages and genetic aspects (primary magmatic versus late-magmatic and/or hydrothermal) of the pipe mineralization.

**Samples**

During a field campaign in 2000, sampling was performed in the vicinity of Merensky's original 1924 discovery site of the "Bushveld platinum", in the Moopetsi river valley on the farm Maandagshoek. The results of this mission were published by Oberthür et al. (2004) and Melcher et al. (2005) and are in part mentioned below to place this current work in context. In a second campaign in 2004, sediments were sampled in rivers at nine localities in the eastern (Groot and Klein Dwars river, Steelpoort river), northern (Mohlosane and Dithokeng river), and western limb (Brakspruit) of the Bushveld Complex (see Figures 1 and 2A). In addition, eluvial material was collected from the western slope of the Onverwacht pipe (Figure 2B), the locality of "platiniferous eluvium and rubble" described by Wagner (1929). Note that at the time of our sampling, the only active platinum mine in the northern part of the eastern Bushveld was the Atok Mine (now Bokoni Mine). As the numerous mining activities currently in operation in the eastern Bushveld had not started, contamination of the samples from this area (eastern Bushveld) by mining can be considered minimal. The main sampling locations are shown in Figure 1 and are described here in brief:

***Locality 1***

*Karee Spruit close to Brits*. Site not sampled by us; sample taken and described by Wilhelm et al. (1997), close to Brits prison where one detrital PGM (one grain of Pt-Pd-Fe alloy intergrown with laurite) was found.

***Locality 2 – western Bushveld***

*Brakspruit* (24°54'56.7"E, 27°12'53.2"S). West of Norton, river north of road bridge. 20 kg of fraction <2 mm.

***Locality 3 – northern Bushveld***

i. *Mohlosane River* (23°58'52.7"E, 28°54'18.0"S and 23°58'54.6"E, 28°54'15.4"S) on farm Zwartfontein. Two samples of 17 + 12 kg <2 mm. Locality illustrated by Cawthorn and Lee (1998, pages 51-53). Probably identical to the Zwartspruit locality described by Wagner (1929, p. 265).
ii. *Dithokeng River* (24°03'57.0"E, 28°58'03.6"S). Small river below (south) of Tweefontein Hill; 15 kg <2 mm. Tweefontein Hill is a famous occurrence of large (cm-sized) sperrylite crystals (e.g. Wagner 1929, Plate II).

***Locality 4 – eastern Bushveld***

i. *Moopetsi River* (ca. 24°36'34.5"E, 30°06'24.3"S) draining south and its tributaries. More than 6000 PGM grains from 701 kg of sample material <2 mm. Locality described by Cawthorn (1999) and Oberthür et al. (2004). The reader is referred to the work on the PGM assemblages published by Oberthür et al. (2004) and Melcher et al. (2005).
ii. *Steelpoort River* (24°42'57.7"E, 30°13'54.3"S). 16 kg <2 mm altogether; chromite-rich concentrate; no PGM extracted.

***Locality 5 – eastern Bushveld***

i. *Klein Dwars River* (24°56'06.3"E, 30°05'58.0"S), close to new bridge across the river; 33 kg <2 mm.
ii. *Dwars River* (24°54'42.5"E, 30°06'11.0"S), close to old bridge near the National Monument (surface outcrop of the UG-1); 24 kg <2 mm.

***Locality 6 – eastern Bushveld***

i. *Groot Dwars River* (25°05'07.0"E, 30°07'17.8"S), farm "Der Brochen", south of dam, 43 kg <2 mm, and
ii. tributary to the east of the Groot Dwars River (25°04'10.3"E, 30°06'47.3"S), 21 kg <2 mm.
iii. *Groot Dwars River* (25°02'51.5"E, 30°07'15.0"S), farm "Der Brochen", ca. one km north of dam, 45 kg <2 mm.

***Locality X – eastern Bushveld***

*Onverwacht Pipe*, western slope (24°39'09.1"E, 30°09'59.3"S). Locality of "platiniferous eluvium and rubble" described by Wagner (1929, p. 65 and 264): "Platinum is present in well-shaped crystals and in

irregular grains and nuggety forms". Note, however, that considerable mining infrastructure was present between ca. 1925 and 1930 on this slope and therefore, some of the material may have originated from the past mining operations. 33 kg of the fraction <2 mm.

**Analytical methods and procedures**

In the field, the sieved fraction <2 mm was panned on site. The samples were screened on site to remove coarser material. After weighing, the finer grained (<6.3 mm; mostly <2 mm only) fractions were panned by hand to obtain heavy mineral pre-concentrates, which were collected in bottles. Further treatment of the heavy mineral pre-concentrates (60 grams to 3.5 kg of black-sand minerals) was performed in the BGR laboratories and comprised panning and sieving into various <2 mm size fractions, and the investigation of the final concentrates under a binocular microscope. The final heavy mineral concentrates mainly consisted of grains of chromite and magnetite (95 to 99%), ilmenite, rutile, zircon, baddeleyite, monazite, PGM and gold. The precious metal grains were extracted from the final


***Figure 2.*** *Field activities: (**A**) Panning of alluvial PGM, Dwars River, Der Brochen, south of dam. (**B**) Onverwacht Pipe (in the background), and eastern slope (foreground) that was sampled for eluvial PGM. Inset: largest (1.87 mm) eluvial PGM grain (Pt-Fe alloy) found at Onverwacht (grain 4/55).*

**Table 1.** Inventory of alluvial PGM identified in sediment samples in rivers draining the Bushveld Complex, and eluvial PGM from the Onverwacht pipe, based on SEM/EDAX data of individual grains.

| Locality | | Brakspruit | Dithokeng River | Mohlosane River | Dwars River | Der Brocken | Onverwacht |
|---|---|---|---|---|---|---|---|
| **Mineral** | **Formula** | **Alluvial** | | | | | **Eluvial** |
| Native Pt | Pt | 2 | 2 | 4 | 1 | 8 | 6 |
| Pt-Pd alloys | Pt-Pd | | | 1 | 1 | 2 | |
| Pt-Fe alloys | Pt-Fe | 2 | | 2 | | 4 | 64 |
| Os-Ru-Rh-Pt alloys | Os-Ru-Rh-Pt | | | | | | 4 |
| Cooperite-Braggite | (Pt,Pd)S | | | 1 | | 5 | |
| Bowieite (?) | $Rh_2S_3$ | | | | | | 2 |
| Laurite | $RuS_2$ | | | | | | 3 |
| Sperrylite | $PtAs_2$ | 1 | 5 | 3 | 2 | 7 | 14 |
| Hollingworthite* | RhAsS* | | | | | | 2 |
| Cherepanovite | RhAs | | | | | | 1 |
| Palladodymite | $(Pd,Ru)_2As$ | | | | | | 1 |
| Stibiopalladinite | $Pd_5Sb_2$ | | | | | 1 | 1 |
| Gold | Au-Ag | | 2 | 5 | | 4 | 1 |
| Σ PGM grains | | 5 | 7 | 11 | 4 | 27 | 98 |

* various PGE-sulfarsenides [(PGE)AsS] – mainly hollingworthite

concentrates by hand, mounted on SEM sample holders and investigated using a scanning electron microscope (SEM) with an attached energy-dispersive X-ray system (EDAX). Following this step of study, grains of interest were embedded in resin and polished sections were prepared for subsequent electron-probe microanalysis (EPMA) using a CAMECA SX100 electron microprobe. Analytical conditions were: Accelerating voltage 20 kV, specimen current 30 nA, and measurement times 10 s. X-ray lines and standards (in brackets) used were: Ru*L*α, Rh*L*α, Os*M*α, Ir*L*α, Au*L*α, Ag*L*β, Ni*K*α, Se*K*α, Te*L*α, Bi*M*α, Sn*L*α (metals), Pt*L*α and Fe*K*α (synthetic $Pt_3Fe$ alloy), Pd*L*α (synthetic PdS), S*K*α (synthetic PtS), As*L*α (synthetic GaAs), Pb*M*α (galena), and Sb*L*α (stibnite). Raw data were corrected using the PAP program (Pouchou and Pichoir, 1991) supplied by CAMECA. Additional corrections were performed for overlaps of Rh, Pd, Ag, Cu, As, and Sb with secondary lines. Detection limits for the elements listed are ca. 0.1 weight %.

## Results

### *Alluvial samples*

The concentrates from the alluvial samples were studied using an SEM. Such investigations are valuable in the study of grain morphologies and thus allow semi-quantitative analytical data for mineral grains to be obtained. However, as the SEM analyses are performed on the surfaces of grains only, some caution has to be exercised regarding the composition of the grains as thin crusts on the grains or overgrowths may produce compositions that differ from those of the internal cores of the grains. Indeed, polished section studies demonstrate that some PGM grains assigned to native Pt or Pt-Fe alloy have cores of cooperite, braggite or in rare cases, sperrylite. This must be taken into consideration regarding the PGM proportions presented in Table 1.

All samples contain discrete PGM grains (3 to 20 grains per sample), and altogether 54 PGM and 11 gold grains were found in the concentrates. PGM grain sizes are mostly in the range from ~50 to 150 µm (maximum diameter 600 µm). The overall PGM proportions are: native Pt, Pt-Pd and Pt-Fe alloys (29 grains; 54%), sperrylite (18 grains; 33%), cooperite/braggite (six grains; 11%), and stibiopalladinite (one grain). Accordingly, nearly all detrital PGM (98%) are Pt minerals, which underlines the fact that Pd-minerals are unstable and are dissolved in the weathering environment (e.g. Oberthür et al., 2004, 2013a; Melcher et al., 2005). Pt-Fe alloy grains are usually unaltered. In contrast, sperrylite and cooperite/braggite grains commonly show either signs of dissolution (e.g. etched pits) or the formation of thin overgrowths of pure Pt.

*Native Platinum* is common in the form of thin surface layers on sperrylite (Figures 3C, D, 4B) or as well-rounded grains (Figures 4D; 5A) which probably contain cores of other PGM. Melcher et al. (2005) reported overgrowths of pure Pt mainly on cooperite/braggite and sperrylite from the eastern Bushveld (Moopetsi valley), and also an overgrowth of native Pt on sperrylite is reported here from the Onverwacht eluvial PGM occurrence (Figure 9C). Furthermore, secondary overgrowths of tiny crystals of native Pt were found on two occasions (Figures 3F; 5E; F). Both textural position and composition indicate a secondary origin for the native platinum.

*Pt-Pd and Pt-Fe alloy* ("ferroan platinum") grains are treated together here as they show considerable overlap geochemically (SEM data) and in physical appearance. Large idiomorphic to hypidiomorphic grains are common and often show no or only minor physical attrition (Figures 3A; B; 4E; F), indicating short transport distances and/or chemical inertness in the fluvial environment.

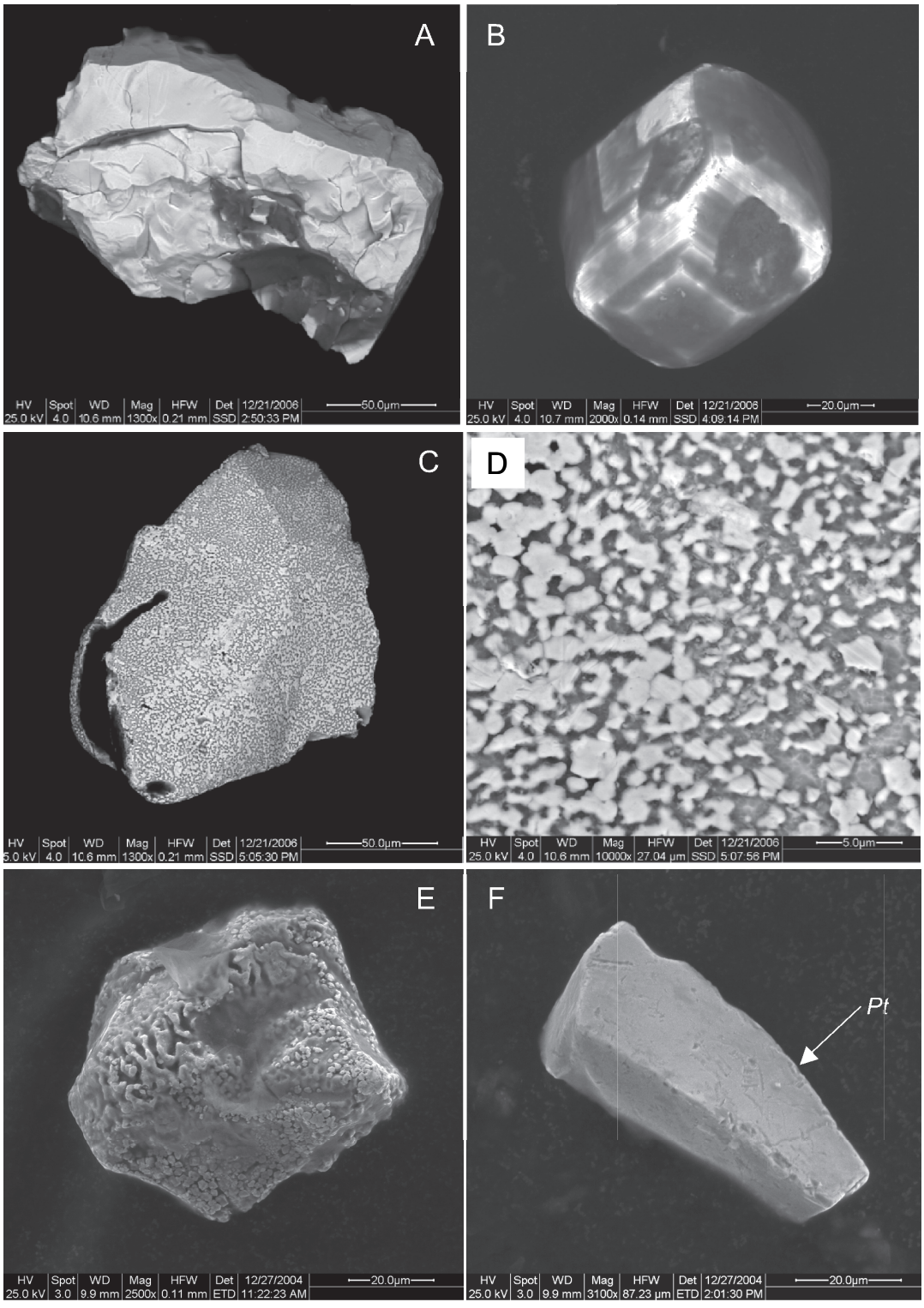


***Figure 3.*** *Scanning electron microscope images (SEM) of individual PGM grains, Der Brochen. (**A**) Crystalline grain of Pt-Pd alloy showing little attrition (grain 12/31). (**B**)Well-crystallized grain of Pt-Fe alloy (grain 12/94). (**C**) Sperrylite grain with overgrowth of Pt platelets (grain 13/44). (**D**) Magnification from C. (**E**) Grain of cooperite/braggite showing surface dissolution (grain 2/77). (**F**) Stibiopalladinite with small dots of pure Pt on the surface (grain 3/04).*

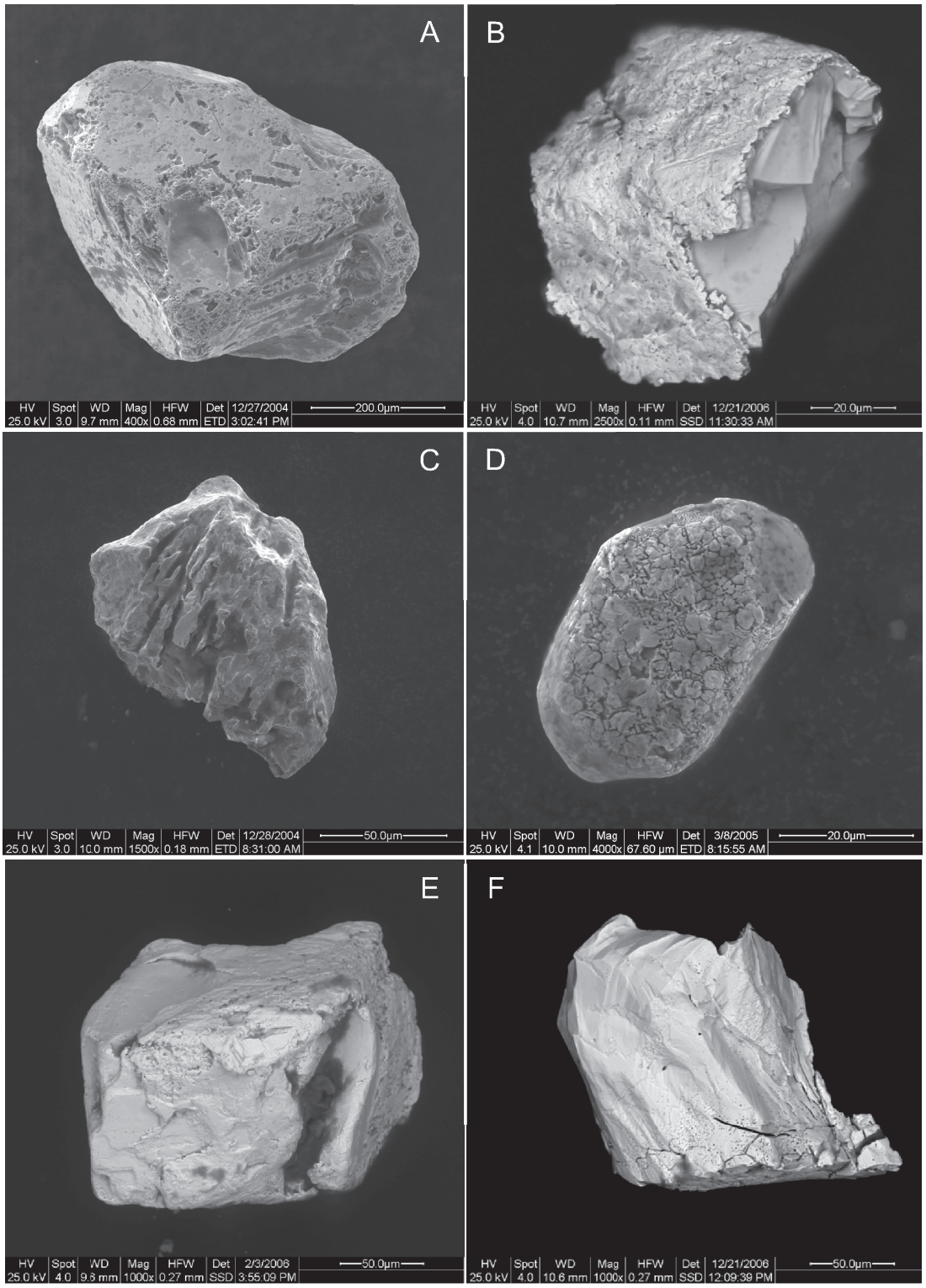


***Figure 4.*** *Scanning electron microscope images (SEM) of individual PGM and gold grains, Mohlosane River (A, C-F) and Dwars River (B). (**A**) Sperrylite grain with abraded surface (grain 3/26). (**B**) Sperrylite with thin surface coating of native Pt (grain 11/27). (**C**) Irregular grain of gold (grain 3/50). (**D**) Native Pt (probably coating on other PGM) (grain 4/06). (**E**) Crystalline grain of Pt-Fe alloy showing little attrition (grain 5/21). (**F**) Fractured grain of Pt-Pd alloy (grain 11/87)*

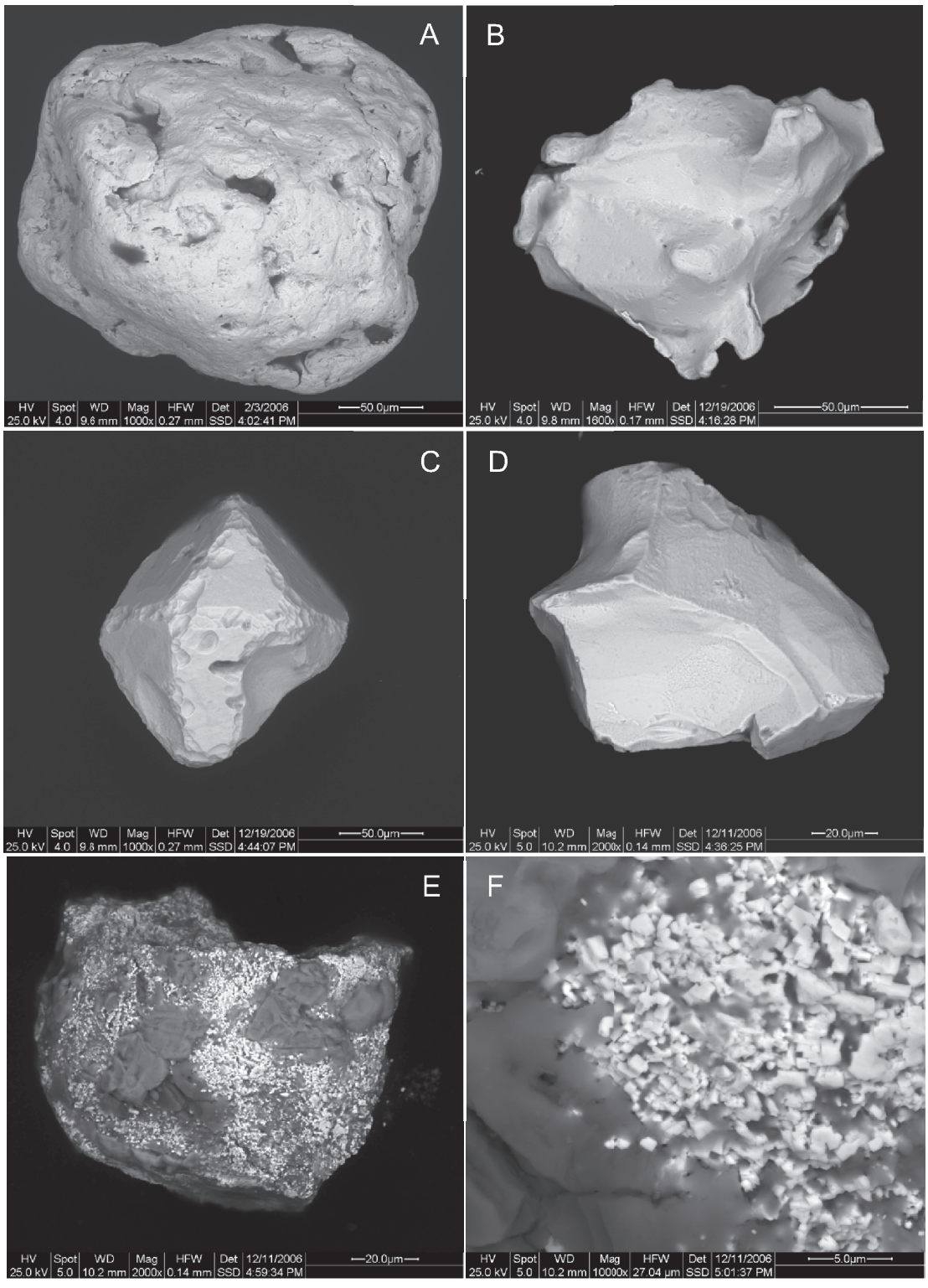


***Figure 5.*** *Scanning electron microscope images (SEM) of individual PGM and gold grains, Dithokeng (A-C) and Brakspruit (D-F) Rivers. (**A**) Well-rounded grain of native Pt (grain 5/32). (**B**) Gold grain with smooth surface (grain 9/98). (**C**) Sperrylite crystal with signs of surface etching (grain 10/12). (**D**) Grain of native Pt with smooth surface (grain 8/24). (**E**) Tiny crystals of native Pt (light grey) on grain of pentlandite (dark grey). Grain 8/14. (**F**) Magnification from E showing crystals of native Pt (light grey).*

**Table 2.** Inventory of eluvial PGM from the Onverwacht pipe identified in polished sections and analyzed by electron microprobe.

| Mineral | Formula | Single grain | Inclusion etc. | No. of grains | No. of analyses |
|---|---|---|---|---|---|
| platinum | Pt | x | | 3 | 3 |
| ferroan platinum | Pt-Fe | x | o | 18 | 26 |
| tetraferroplatinum | PtFe | x | | 2 | 2 |
| tulameenite | $Pt_2FeCu$ | x | o | 21 | 27 |
| osmium | Os | | o | | 1 |
| ruthenium | Ru | | o | | 3 |
| rhodium | Rh | x | | 1 | 1 |
| sperrylite | $PtAs_2$ | x | o | 10 | 11 |
| cherepanovite | RhAs | x | | 2 | 2 |
| ruthenarsenite | RuAs | x | | 2 | 2 |
| rhodarsenide | $(Rh,Pd)_2As$ | x | | 1 | 1 |
| stumpflite (?) | PtSb | x | o | 1 | 2 |
| stibiopalladinite | $Pd_5Sb_2$ | x | o | 2 | 15 |
| Rh-genkinite | $(Pt,Pd,Rh)_4Sb_3$ | x | o | 3 | 4 |
| ruarsite | RuAsS | | o | | 2 |
| hollingworthite | RhAsS | x | o | 2 | 15 |
| irarsite | IrAsS | | o | | 2 |
| platarsite | PtAsS | x | o | 2 | 3 |
| atokite | $Pd_3Sn$ | | o | | 2 |
| Rh-isomertieite | $(Pd,Rh)_{11}Sb_2As_2$ | x | | 1 | 1 |
| *unnamed* | $Pd_3TeBi$ | | o | | 1 |
| *unnamed* | RhSb | x | | 1 | 1 |
| *unnamed* | (Pt,Pd,Rh)-oxide | x | | 1 | 1 |
| **Σ analyses** | | | | | **128** |

Ideal formulae after Cabri (2002).

*Sperrylite* [$PtAs_2$] is up to 600 µm in size (Figure 4A) and is occasionally idiomorphic (Figure 5C), generally showing no signs of chemical attack. Overgrowths of native Pt are quite common (Figures 3C; D; 4D).

*Cooperite/braggite* [(Pt,Pd)S] grains generally display signs of surface dissolution (Figure 3E) indicating that they are chemically unstable in the fluvial environment, corroborating the statements of Melcher et al. (2005) and Oberthür et al. (2004, 2013a).

One hypidiomorphic, fresh grain of *stibiopalladinite* [$Pd_5Sb_2$] was detected in a sample from Der Brochen (Figure 3F). Some tiny specks of native Pt are present on the surface of this grain.

*Gold* grains generally show smooth surfaces and often have slightly bent corners (Figure 5B). More compact grains are also present (Figure 4C).

### *Eluvial sample*

From 33 kg of eluvial material (<2 mm) collected at Onverwacht, ca. 150 PGM grains were extracted (97 grains were studied by SEM). Grain sizes are mainly in the range 100 to 300 µm. The PGM assemblage comprises grains of Pt-Fe alloys (66%), sperrylite (14%) and a suite of rarer PGM including stibiopalladinite, hollingworthite, laurite, and some additional PGE arsenides and very rare PGE sulfides (Table 1). Idiomorphic single crystals especially of Pt-Fe alloy predominate, however, many grains are composite as well. Virtually no physical damage or chemical alteration of the PGM grains reflects their direct derivation from the Onverwacht pipe (transport distance < 50 m).

### *Scanning electron microscopy (SEM) observations*

Grains of Pt-Fe alloy ("ferroan platinum") are the most frequent PGM identified. Their sizes are usually in the range 100 to 300 µm, however, larger grains are also present including one crystalline grain of Pt-Fe alloy with a maximum diameter of 1.87 mm. Monomineralic, idiomorphic cubes with no signs of attrition are common (Figures 6D; E), as are polymineralic grains consisting of simple to complex intergrowths of Pt-Fe alloy with laurite [$RuS_2$] and ilmenite [$FeTiO_3$] (Figure 6B), laurite and cherepanovite [RhAs] (Figure 6C), Ru-Os alloy (Figure 6F), laurite, hollingworthite [RhAsS] and cherepanovite (Figure 7A), and laurite and hollingworthite (Figure 7E). Further PGM documented using the SEM comprise compact sperrylite (Figure A) and stibiopalladinite (Figure 7B), both displaying slightly etched features on their surfaces, as well as native Pt (Figure 7D) and one grain of possible bowieite [$Rh_2S_3$].

### *Electron microprobe investigation*

The EPMA work confirmed the predominance of Pt-Fe alloy grains ("ferroan platinum"), and the suite of PGM analyzed is presented in Table 2. Many of the Pt-Fe alloy grains were found to be polyphase, showing coarse intergrowths with a number of other PGM,

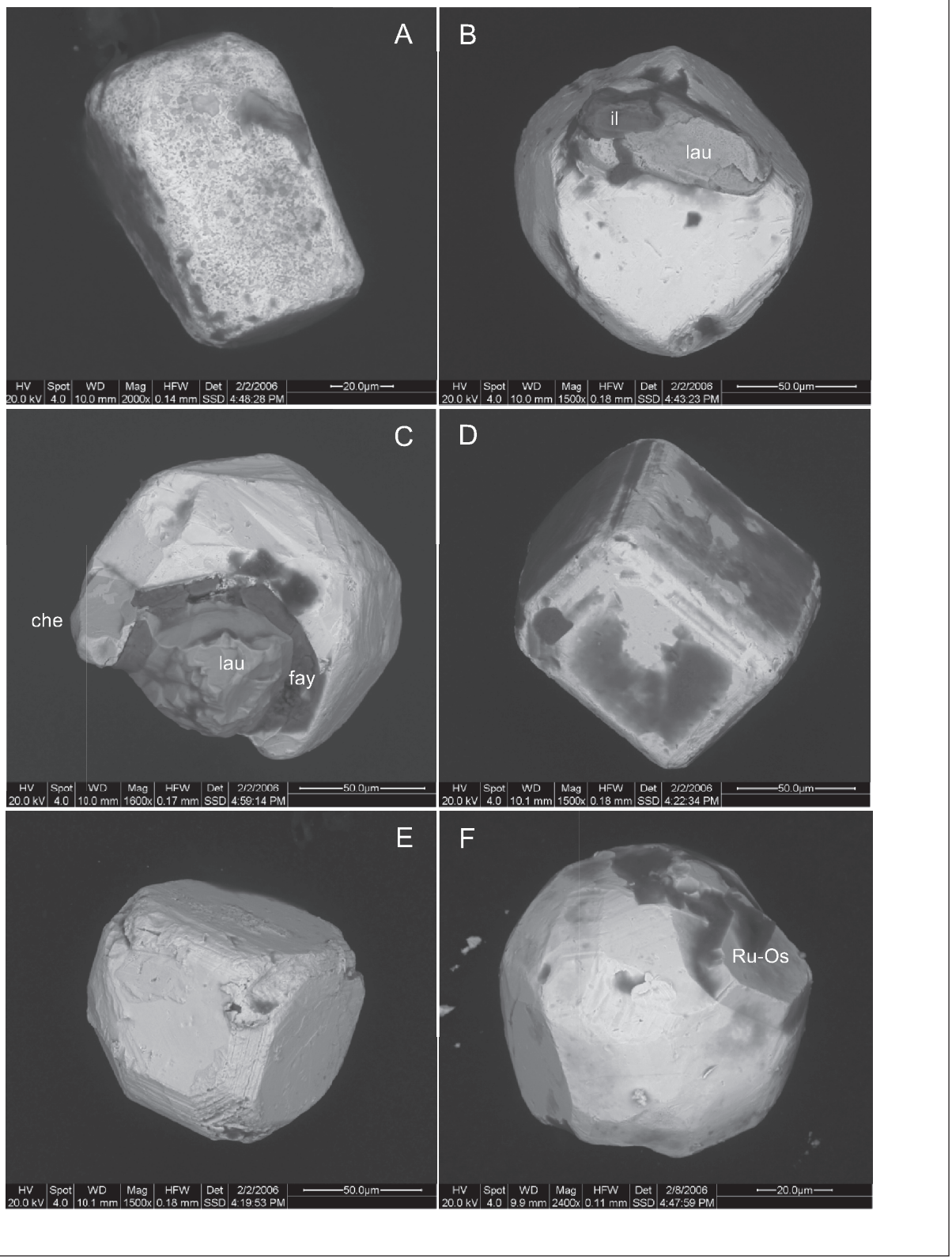


***Figure 6.*** *Scanning electron microscope images (SEM) of individual eluvial PGM grains, Onverwacht. (**A**) Sperrylite with etched and pitted surface (grain 4/71). (**B**) Well-crystallized grain of Pt-Fe alloy (light grey) intergrown with laurite (medium grey, lau) and ilmenite (dark grey, il). Grain 4/75. (**C**) Well-crystallized grain of Pt-Fe alloy (light grey) intergrown with cherepanovite (che) and laurite (lau) which is rimmed by fayalite (fay). Grain 4/76. (**D**) Cubic crystal of Pt-Fe alloy showing no attrition but thin surface coatings (darker) of secondary Fe-hydroxides (grain 4/56). (**E**) Fresh cubic crystal of Pt-Fe alloy showing (grain 4/55). (**F**) Well-crystallized grain of Pt-Fe alloy (light grey) with attached platelet (medium grey, top right) of a Ru-Os alloy (grain 6/07).*

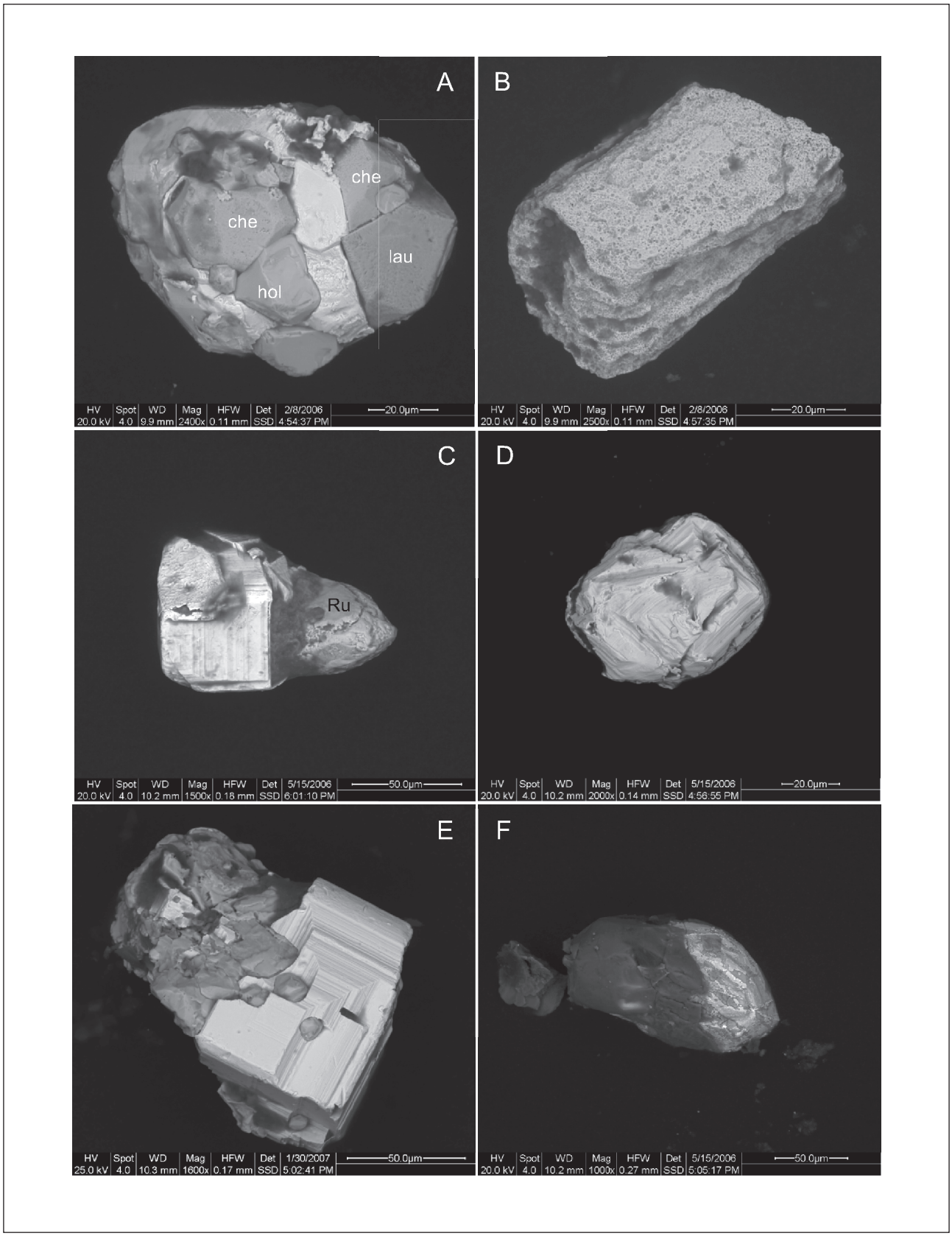


***Figure 7.*** *Scanning electron microscope images (SEM) of eluvial PGM grains, Onverwacht. (**A**) Intergrowth of Pt-Fe alloy (lightest grey), laurite (lau), hollingworthite (hol) and cherepanovite (che). Grain 6/08. (**B**). Stibiopalladinite with etched, pitted surface (grain 6/09). (**C**) Intergrowth of a crystal of Pt-Fe alloy (cube with striped surface, lightest grey), and Ru (darker). Grain 6/52. (**D**) Well-crystallized grain of pure Pt (grain 6/19). (**E**) Intergrowth of a crystal of Pt-Fe alloy (cube with striped surface, lightest grey), and hollingworthite (medium grey). Grain 6/54. (**F**) Bowieite (light grey, right) intergrown with Mg-silicate (dark, left). Grain 6/20.*

**Table 3.** Electron microprobe analyses of PGE alloys, Onverwacht eluvial. (114) Native platinum, (20 + 31) Ferroan platinum, (30) Tetraferroplatinum [PtFe], (21 + 62) Tulameenite [$Pt_2CuFe$], (105) Osmium, (98) Ruthenium, (92) Rhodium.

| No. | 114 | 20 | 31 | 30 | 21 | 62 | 105 | 98 | 92 |
|---|---|---|---|---|---|---|---|---|---|
| | | | | | **Weight percent** | | | | |
| Pt | 89.93 | 85.78 | 83.87 | 77.43 | 76.57 | 75.51 | 26.34 | 17.00 | 42.45 |
| Pd | | | | | | | | | 0.23 |
| Os | | | | | | | 48.42 | 17.90 | |
| Ir | | 0.76 | 0.61 | 0.58 | 0.45 | | | 12.84 | 0.66 |
| Ru | | | | | | | 9.21 | 46.48 | 14.86 |
| Rh | 0.22 | 0.42 | | | | | | 1.05 | 34.28 |
| Fe | 1.47 | 10.72 | 11.47 | 13.88 | 13.30 | 11.14 | 3.76 | 2.23 | 1.53 |
| Cu | 0.08 | 0.75 | 0.70 | 2.68 | 5.40 | 10.42 | 0.29 | 0.16 | 1.82 |
| Ni | 0.08 | 0.68 | 1.73 | 3.36 | 3.00 | 0.86 | 0.37 | 0.24 | |
| S | 0.08 | | | | 0.09 | | | | |
| As | 0.36 | 0.01 | 0.02 | | 0.01 | 0.02 | | | |
| Te | | | | | | | | | |
| Sb | | 0.14 | 0.17 | 0.19 | 0.26 | 0.32 | 0.10 | | 0.11 |
| Bi | | 0.10 | | | 0.09 | | | | |
| Sn | | | | | 0.12 | 0.14 | | | |
| Total | 92.22 | 99.36 | 98.57 | 98.12 | 99.29 | 98.41 | 99.44 | 97.90 | 95.94 |
| | | | | | **Atomic proportions** | | | | |
| Pt | 0.923 | 1.323 | 1.263 | 1.059 | 1.127 | 1.006 | 0.22 | 0.114 | 0.286 |
| Pd | | | | | | | | | 0.003 |
| Os | | | | | | | 0.413 | 0.123 | |
| Ir | | 0.012 | 0.009 | 0.008 | 0.007 | | 0.092 | 0.087 | 0.004 |
| Ru | | | | | | | 0.148 | 0.601 | 0.193 |
| Rh | 0.004 | 0.012 | | | | | | 0.016 | 0.438 |
| Fe | 0.053 | 0.577 | 0.604 | 0.663 | 0.683 | 0.519 | 0.109 | 0.052 | 0.036 |
| Cu | 0.003 | 0.036 | 0.032 | 0.113 | 0.018 | 0.426 | 0.007 | 0.003 | 0.038 |
| Ni | 0.003 | 0.035 | 0.087 | 0.153 | 0.147 | 0.038 | 0.010 | 0.005 | |
| S | 0.005 | | | | 0.008 | | | | |
| As | 0.009 | | 0.001 | | 0.000 | 0.001 | | | |
| Te | | | | | | | | | |
| Sb | | 0.004 | 0.004 | 0.004 | 0.006 | 0.007 | | | 0.001 |
| Bi | | 0.001 | | | 0.001 | | | | |
| Sn | | | | | 0.003 | 0.003 | | | |

mainly stibiopalladinite (Figures 8B; C), hollingworthite (Figures 8B; C; 9D), Rh-bearing genkinite (Figure 8D), cherepanovite (Figures 8E; 9D), sperrylite (Figure 9A), platarsite (Figure 9A), isomertieite (Figure 9D) and tetraferroplatinum (Figure 8D). Chemically, most of the Pt-Fe alloys approach isoferroplatinum [$Pt_3Fe$] in composition (Table 3), however, a number of grains are of tetraferroplatinum [PtFe] (e.g. Figure 8D; Table 3). Many of the Pt-Fe alloy grains show incipient to pervasive replacement by tulameenite [Pt(Cu,Fe)] (Figures 8C, 9B, F, H), indicating an overprint by late-phase copper-rich fluids. Inclusions comprise needles of ruthenium (Figure 8E) and round grains of osmium (Figure 9A).

Some grains of porous, pure platinum were also encountered (Figure 9E), as well as grains of sperrylite (Figure 8F). In one case, a thin rim of pure Pt was observed on an idiomorphic grain of sperrylite (Figure 9C). The electron microprobe work predominantly concentrated on the rarer PGM. Selected analyses of the various PGM are presented in Tables 3 and 4.

*Native Platinum* [Pt] in the form of flat, homogeneous grains with rounded corners reach up to 80 µm in diameter. Pt is also present enclosed in tetraferro-platinum, as porous single grains (Figure 9E) and as a porous rim around idiomorphic sperrylite (Figure 9C; analysis Table 3 no. 1).

*Ferroan platinum* [$Pt_{2-3}Fe$] appears as up to 150 µm sized, rounded and mostly homogeneous single grains commonly more or less replaced by tulameenite on the outer rims. Flat or round inclusions in tulameenite are also present. In rare cases, ferroan platinum forms laminar intergrowths with tetraferroplatinum (Figure 8D; Table 3, nos. 20 and 31).

*Tetraferroplatinum* [PtFe] reaches 80 µm in size. Tabular grains with rounded edges predominate, and the laminar intergrowths with ferroan platinum (Figure 8D) have been described already. Inclusions consist of hollingworthite/irarsite, and open cracks may be filled by native platinum and sperrylite (analysis Table 3, no. 30).

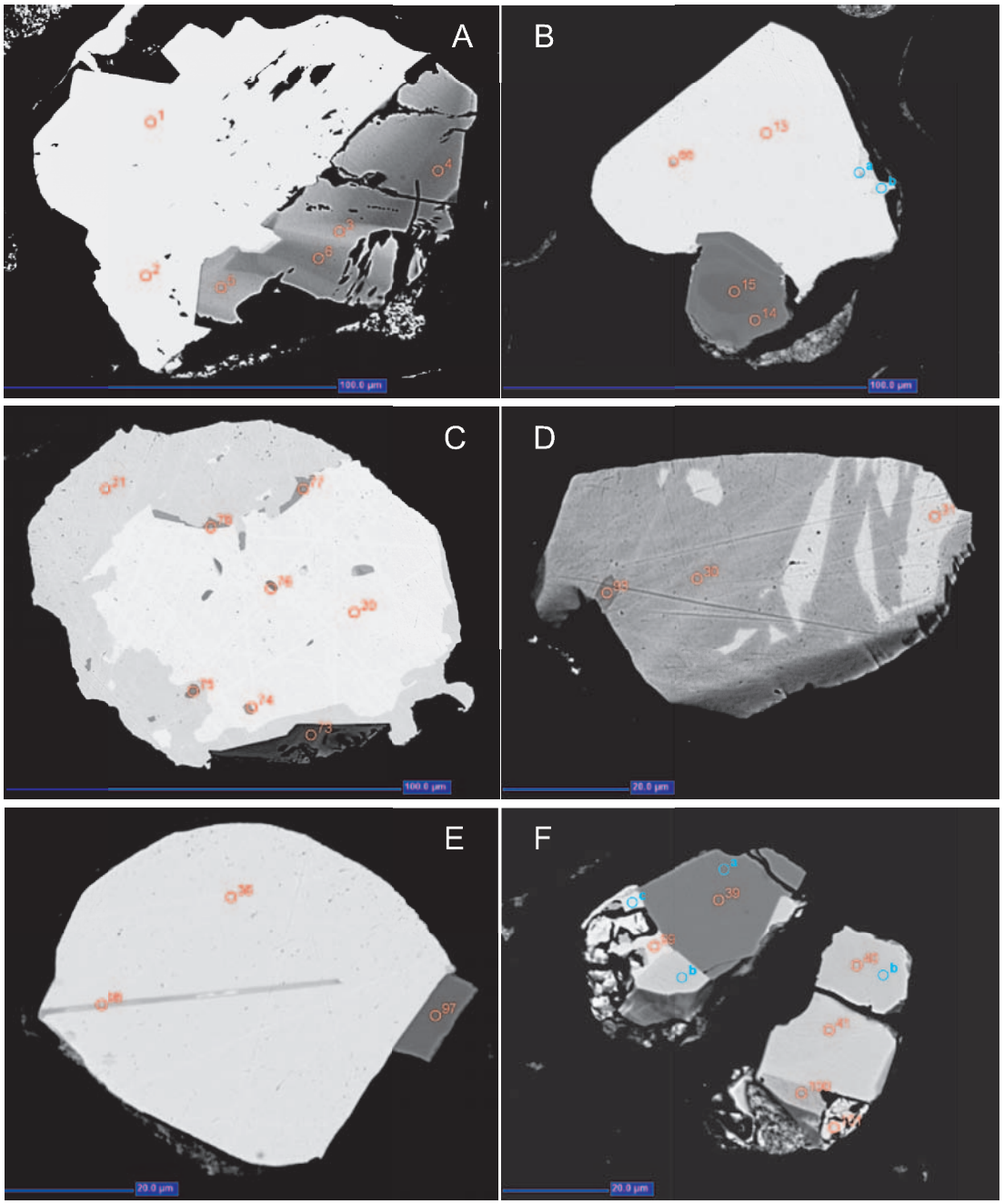


***Figure 8.*** *Backscatter electron (BSE) images of eluvial PGM from Overwacht in polished sections (AS 7605). (**A**) Tulameenite (1,2; white area) intergrown with ruarsite (3, 5; light grey) and hollingworthite (4, 6; dark grey). (**B**) Ferroan platinum (13) with tiny inclusion of stibiopalladinite (66; dark) and intergrown with zoned hollingworthite (14, 15). (**C**) Ferroan platinum (20; white) partly rimmed by tulameenite (21; light grey), with inclusions of stibiopalladinite (74-78; dark grey), and intergrown with hollingworthite (73; dark grey, at bottom). (**D**) Oval grain of tetraferroplatinum (30; grey) in flame-like intergrowth with ferroan platinum (31; light) and an idiomorphic inclusion of Rh-genkinite (93; dark, left part of grain). (**E**) Roundish grain of ferroan platinum (36; white) with a lamella of ruthenium (98; grey). Attached is an idiomorphic grain of cherepanovite (97; dark grey, right side of grain). (**F**) Grain top left: intergrowth of ruthenarsenite (30; darkgrey ) and Rh-genkinite (99; light grey). Grain bottom right: broken grain of sperrylite (40, 41; light) intergrown with stibiopalladinite (100; grey) and Sb-bearing platinum [$Pt_{80}Sb_{20}$] (101; white; possible stumpflite?).*

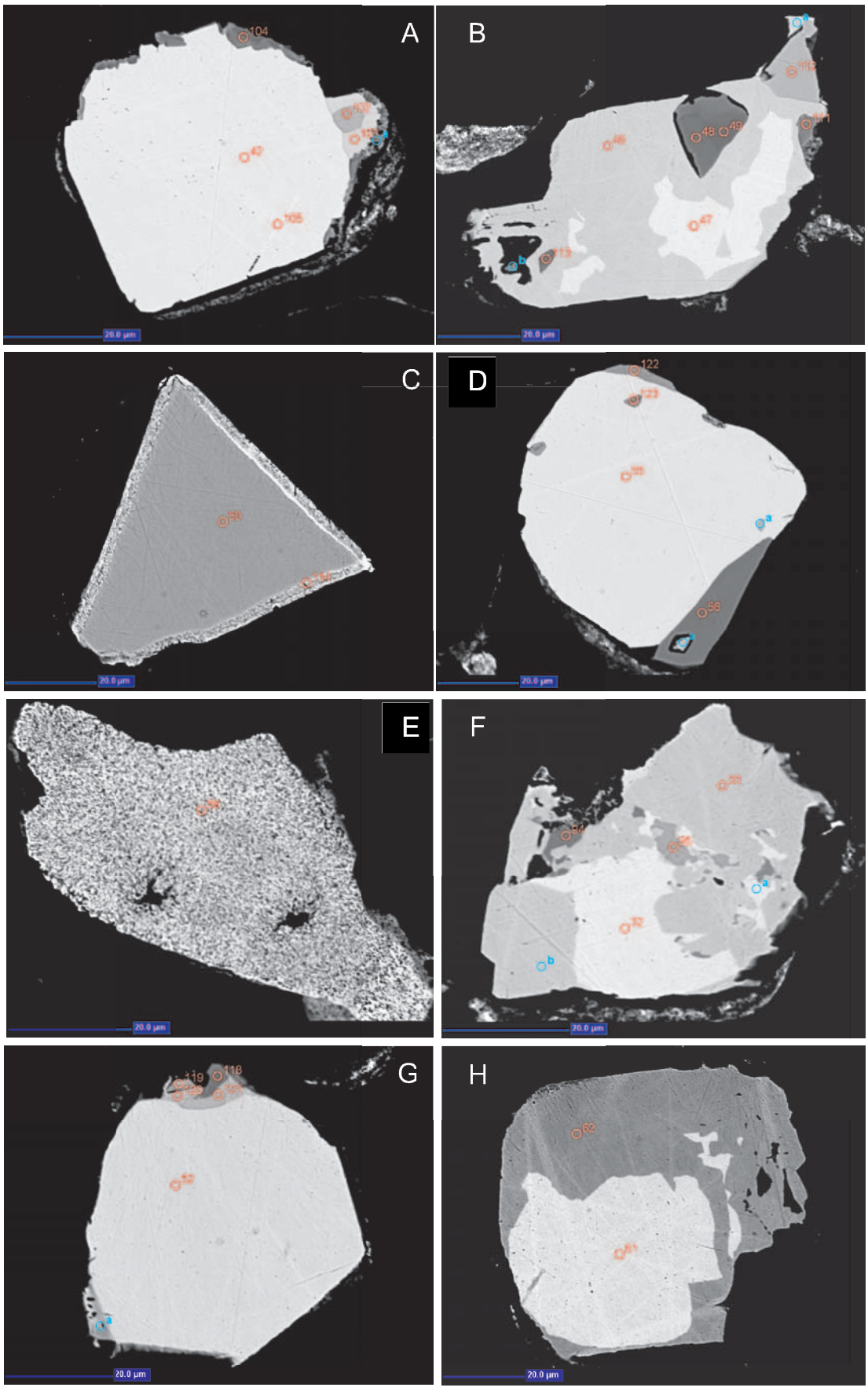
A
B
C
D
E
F
G
H

*Tulameenite* [$Pt_2FeCu$] is up to 150 µm in diameter, often intergrown with or replacing ferroan platinum, and in some cases contains inclusions of stibiopalladinite (Figures 9F; 9H; Table 3, nos. 21 and 62).

*Native osmium* [Os] was detected included in ferroan platinum. Notably, the mineral contains appreciable amounts of Ru (9 weight %) and Pt (26 weight %; Table 3, no. 105).

*Native ruthenium* [Ru] is found up to 10 µm in size intergrown with ferroan platinum along the latter's periphery. In addition, one 50 µm long lamella of ruthenium was observed in ferroan platinum (Figure 8E; Table 3, no. 98). According to Cabri (2002), ruthenium forms a complete solid solution series with osmium and partly with iridium. However, the analyses of the present study all plot in the ternary systems Ru-Ir-Pt, Ru-Ir-Rh, and Ru-Os-Pt (Harris and Cabri, 1991).

*Native rhodium* [Rh] was detected once in the form of a 10 µm, lobate and porous grain overgrowing tulameenite (Table 3, no. 92).

*Sperrylite* [$PtAs_2$] reaches up to 150 µm in size. The grains are mostly tabular, internally mostly homogeneous, and commonly also fractured. Predominantly, single grains with stoichiometric composition are encountered which occasionally display overgrowths by ferroan platinum (Figure 9A), tulameenite or stibiopalladinite. An idiomorphic grain of sperrylite showing replacement by native platinum is shown in Figure 9C.

*Cherepanovite* [RhAs] grains are tabular and up to 40 µm in diameter, intergrown with ferroan platinum (Figures 8E; 9D). Cherepanovite carries significant ruthenium content (24 weight %; Table 4, no. 97).

*Ruthenarsenite* [RuAs] grains up to 20 µm in diameter are tabular and were found intergrown with sperrylite or Rh-genkinite (Figure 8F; Table 4, no. 69).

*Rhodarsenide* [$(Rh,Pd)_2As$] in the form of small (20 µm) tabular grains was identified intergrown with ferroan platinum (Table 4, no. 96).

Notably, all the above mentioned PGE arsenides were reported in the alluvial PGM assemblage from Maandagshoek (Oberthür et al. 2004, Melcher et al. 2005).

*Stumpflite* [PtSb] (?) was found as up to 10 µm inclusions in sperrylite and as a broken single grain intergrown with sperrylite and stibiopalladinite (Figure 8F; Table 4, no. 79).

*Stibiopalladinite* [$Pd_5Sb_2$] is quite common in the PGM assemblage. The mineral occurs as up to 10 µm tabular single grains which may be intergrown with sperrylite. Further, small, roundish to tabular stibiopalladinite inclusions are present in ferroan platinum and tulameenite. Microprobe analyses reveal stoichiometric compositions [$Pd_5Sb_2$]; no As was detected. One rare grain was Pt-, Rh- and As-bearing [$(Pd_{2.50}Rh_{1.88}Pt_{.29}Fe_{.07})_{4.74}(Sb_{1.57}As_{0.67})_{2.24}$] (Figure 9F), chemically tending into the direction of mertieite (I) [$Pd_{11}(Sb,As)_4$].

*Rh-genkinite* [$(Pt,Pd,Rh)_4Sb_3$] was found intergrown with tetraferroplatinum and ruthenarsenite, or as thin rims on sperrylite (Figures 8D; 9A; Table 4, no. 93).

The sulpharsenides of Rh, Ir and Pt (hollingworthite, irarsite and platarsite) crystallize in the cubic system and form a complete solid solution series (Cabri, 2002). Naming these minerals after their end-members in the system follows the 33% rule (Nickel, 1992). Ruarsite is monoclinic and forms a solid solution with osarsite [OsAsS], and uptake of Rh, Ir and Pt by ruarsite is generally minimal.

*Ruarsite* [RuAsS] lamellae were detected in hollingworthite (Figure 8A) with significant Rh, Ir and Pt contents.

*Hollingworthite* [RhAsS] grains up to 100 µm in diameter have tabular or cubic shapes. The mineral is often intergrown with ferroan platinum or tulameenite and is also found as roundish inclusions in Pt-Fe alloy grains. Many grains are distinctly zoned grading into ruarsite, platarsite and irarsite (Figures 8A; B; C).

*Irarsite* [IrAsS] forms small lobate grains up to 10 µm in diameter, partly zoned and intergrown with

***Figure 9.*** *BSE images of eluvial PGM from Overwacht, polished section AS 7605. (**A**) Slightly rounded grain of ferroan platinum (42; white) with drop-like, small inclusion of osmium (105), intergrown on right side of grain with sperrylite (102; grey) which is rimmed by Rh-genkinite (103; light grey) and platarsite (104; dark). (**B**) Irregular grain of tulameenite (46; medium grey) surrounding relics (?) of ferroan platinum (47; light grey), hollingworthite inclusions (48, 49, 113; dark grey), and intergrowth with sperrylite (112; grey, top right) and platarsite (111; middle grey, on right border of grain.). (**C**) Idiomorphic grain of sperrylite (50; medium grey) rimmed by pure platinum (114; white). (**D**) Ferroan platinum (55; white) with inclusion of hollingworthite (123; dark grey), rimmed by Rh-bearing isomertieite (122; light grey, top) and intergrown with cherepanovite (56; dark grey, bottom right). (**E**) Porous, pure native platinum (58). (**F**) Complex intergrowth of ferroan platinum (32; light grey) and tulameenite (33; medium grey), and inclusions of stibiopalladinite (94, 95; darker grey). (**G**) Ferroan platinum (52; light grey) intergrown with (at top of grain) tulameenite (120; medium grey,), Rh-genkinite (121; grey), unnamed RhSb (118; dark grey), and probable Pt-Rh-Pd-oxide (119; dark grey). (**H**) Relict of ferroan platinum (61; light grey) replaced by tulameenite (62; medium grey).*

**Table 4.** Electron microprobe analyses of various PGM, Onverwacht eluvial. (69) Ruthenarsenite [RuAs], (93) Rh-genkinite [$(Pt,Pd,Rh)_4Sb_3$], (96) Rhodarsenide [$(Rh,Pd)_2As$], (97) Cherepanovite [RhAs], (79) Stumpflite (?) [PtSb], (122) Rh-isomertieite [$(Pd,Rh)_{11}Sb_2As_2$], (82) unnamed [$Pd_3TeBi$], (118) unnamed [RhSb], (119) unnamed [(Pt,Pd,Rh)-oxide].

| No. | 69 | 93 | 96 | 97 | 79 | 122 | 82 | 118 | 119 |
|---|---|---|---|---|---|---|---|---|---|
| | | | | | **Weight percent** | | | | |
| Pt | 2.72 | 35.98 | 0.27 | 0.66 | 85.02 | 1.47 | 5.51 | 1.46 | 52.24 |
| Pd | 0.48 | 12.96 | 31.13 | | | 37.11 | 43.48 | | 12.87 |
| Os | | | | | | | | | |
| Ir | 2.43 | 0.54 | | | 0.29 | | | 1.50 | 1.77 |
| Ru | 34.19 | | | 23.68 | | | | | |
| Rh | 17.93 | 10.66 | 40.26 | 33.05 | 1.34 | 27.74 | | 44.83 | 13.46 |
| Fe | 0.71 | 0.41 | 0.30 | 0.74 | 0.75 | 0.44 | 0.55 | 0.40 | 0.89 |
| Cu | | 1.33 | 0.23 | | | | 0.61 | | |
| Ni | 0.69 | 0.59 | | | | | 0.20 | | 0.13 |
| S | | | | | | | | | 0.22 |
| As | 38.69 | 0.61 | 16.88 | 37.36 | 0.47 | 10.02 | | 0.13 | 4.29 |
| Te | | | 1.30 | | | | 16.66 | | |
| Sb | 0.23 | 37.50 | 3.20 | 3.22 | 6.89 | 21.59 | | 53.52 | 1.66 |
| Bi | | | | | 0.08 | | 33.42 | | |
| Sn | | 0.24 | 0.10 | | | 0.18 | | 0.67 | 0.36 |
| Total | 98.07 | 100.82 | 93.67 | 98.65 | 94.84 | 98.55 | 100.37 | 102.51 | 88.25 |
| | | | | | **Atomic proportions** | | | | |
| Pt | 0.026 | 1.678 | 0.004 | 0.006 | 1.654 | 0.12 | 0.188 | 0.017 | 0.425 |
| Pd | 0.008 | 1.112 | 0.918 | | | 5.528 | 2.724 | | 0.192 |
| Os | | | | | | | | | |
| Ir | 0.023 | 0.025 | | | 0.006 | | | 0.017 | 0.015 |
| Ru | 0.622 | | | 0.427 | | | | | |
| Rh | 0.321 | 0.942 | 1.226 | 0.586 | 0.049 | 4.273 | | 0.962 | 0.208 |
| Fe | 0.023 | 0.066 | 0.017 | 0.024 | 0.051 | 0.125 | 0.066 | 0.016 | 0.025 |
| Cu | | 0.190 | 0.011 | | | | 0.064 | | |
| Ni | 0.023 | 0.091 | | | | | 0.022 | | 0.004 |
| S | | | | | | | | | 0.011 |
| As | 0.951 | 0.074 | 0.706 | 0.909 | 0.024 | 2.120 | | 0.004 | 0.091 |
| Te | | | 0.032 | | | | 0.870 | | |
| Sb | 0.004 | 2.802 | 0.082 | 0.048 | 0.215 | 2.804 | | 0.971 | 0.022 |
| Bi | | | | | | | 1.066 | | |
| Sn | | 0.018 | 0.003 | | 0.001 | 0.023 | | 0.012 | 0.005 |

hollingworthite as inclusions in tetraferroplatinum or filling fractures in tulameenite.

*Platarsite* [PtAsS] usually shows a significant content of Rh and Ru (Figure 9A). One analysis arrived at the composition $[(Pt_{.33}Ru_{.31}Rh_{.20}Ir_{.16}Fe_{.04})_{1.02}(As_{.98}Sb_{.01})_{.99}S_{.97}]$.

*Atokite* [$Pd_3Sn$] forms a complete solid solution series with rustenburgite [$Pt_3Sn$]. Small (5 µm) oriented lamellae of atokite having the composition $[(Pd_{1.64}Pt_{1.06}Fe_{.19}Cu_{.19}Ni.0_3)_{1.02}(Sn_{.87}Sb_{.02})_{.89}]$ were observed in tulameenite.

*Rh-isomertieite* [$(Pd,Rh)_{11}Sb_2As_2$]. One 20 µm long grain with elevated Rh contents $[(Pd_{5.53}Rh_{4.27}Pt_{.12}Fe_{.12})_{10.04}(Sb_{2.81}Sn_{.02})_{2.83}As_{2.12}]$ was detected overgrowing ferroan platinum.

*Unnamed* [$Pd_3TeBi$] was found in the form of a 10 µm large platy inclusion in tulameenite (Table 4, no. 82).

*Unnamed* [RhSb]. One ca. 10 µm tabular grain with rounded corners, intergrown with genkinite (Figure 9G; Table 4, no. 118) was located. A chemically similar grain with a Rh/Sb ratio of one was identified, intergrown with stibiopalladinite and ferroan platinum, in an ore sample from the Mooihoek pipe (own data; AS 7915b).

*Unnamed* [(Pt,Pd,Rh)-oxide]. One small (5 µm) tabular grain intergrown with tulameenite (Figure 9G; Table 4, no. 119) was identified. Notably, a number of unnamed Pd- and Ru-/Rh- oxides or hydroxides were described by Melcher et al. (2005) in their study of detrital PGM from the eastern Bushveld.

In the small sample volume (33 kg of eluvial material <2 mm), the suite of eluvial PGM observed basically

represents the PGM assemblage described previously from the Onverwacht pipe proper by Genkin et al. (1966), Cabri et al. (1977a; b; c), Rudashevsky et al. (1992) and Zaccarini et al. (2002). Included are also the Onverwacht pipe type locality minerals genkinite, irarsite and platarsite, as well as some additional and possibly new PGM. Furthermore, most of the relatively rare PGM detected in the suite of eluvial grains from Onverwacht were also reported from the detrital PGM assemblage from the Moopetsi river on the farm Maandagshoek (Oberthür et al. 2004, Melcher et al. 2005), indicating that many of the latter grains originate from platiniferous pipes and not from the Merensky or UG-2 reefs.

**Summary and conclusions**

The present work provides an initial description of detrital PGM in alluvial sediments of rivers draining the Bushveld Complex, and in eluvial concentrations at the Onverwacht platiniferous pipe. All rivers studied draining the Bushveld Complex contain at least some grains of detrital PGM. However, sub-economic alluvial and eluvial concentrations (see Wagner, 1929) are probably only attained in places where a combination of particular circumstances (proximity of sources, particular sedimentological conditions and history) are met.

The suite of detrital PGM encountered comprises native Pt, Pt-Pd and Pt-Fe alloys, sperrylite, cooperite/braggite, and rare stibiopalladinite. This PGM assemblage distinctly contrasts to the suite of PGM in the pristine, sulfide-bearing mineralization of the Merensky, UG-2 and Platreef, the assumed sources of the detrital PGM. PGM in the pristine Bushveld ores mainly comprise sperrylite [PtAs2], cooperite/braggite [(Pt,Pd,Ni)S], (Pt,Pd)-bismuthotellurides, PGE-sulfarsenides and variable quantities of Pt-Fe alloys (e.g. Kinloch, 1982; Schouwstra et al., 2000; Cawthorn et al., 2002; Osbahr et al., 2013; 2014; Junge et al., 2014). In addition, substantial proportions of PGE (mainly Pd and Rh) are hosted in pentlandite (e.g. Osbahr et al., 2013; 2014; Junge et al., 2014).

Specifically, PGE-bismuthotellurides and -sulfarsenides, common in the primary ores, are missing in the assemblage of detrital PGM in the fluvial environment. Nearly all detrital PGM (98%) are Pt minerals, corroborating earlier findings (e.g. Wagner (1929) on the Merensky reef of the Bushveld, and Evans et al. (1994) and Oberthür et al. (2003; 2013b) on surface ores of the Great Dyke, that Pd-dominated PGM are unstable and are dissolved in the supergene environment and that Pd is more mobile than Pt and is dispersed during weathering.

Pt-Fe alloy grains are usually unaltered. In contrast, sperrylite and cooperite/braggite grains commonly show either signs of dissolution (e.g. etch pits) or the formation of thin overgrowths of pure native Pt. Sperrylite grains are relict minerals with multiple possible origins (platiniferous pipes, Merensky and UG-2 reefs), thus indicating that sperrylite is generally stable in the supergene environment. Many of the cooperite/braggite grains show distinct features of external corrosion and partial internal leaching along irregular corrosion channels (Oberthür et al., 2004; 2013a; Melcher et al., 2005), indicating that cooperite/braggite grains are progressively disintegrated in the course of prolonged oxidation (i.e. they are "metastable" in the placers). Further, (Pt,Pd)-bismuthotellurides and PGE-sulfarsenides, common in the pristine ores, are components that are missing in the suite of detrital PGM. Apparently, these minerals disintegrated chemically and physically during weathering and mechanical transport. This work further demonstrates that the order of decreasing stability in the supergene environment is as follows: (1) Pt-Fe alloys (very stable) → (2) sperrylite (stable) → (3) cooperite/braggite (variably stable/"meta-stable") → (4) PGE-bismuthotellurides and PGE-sulfarsenides (unstable).

The high proportion of Pt-Fe alloy grains is conspicuous. The origin of Pt-Fe alloy ("ferroan platinum"), the most abundant PGM in most placers worldwide (Cabri et al., 1996; Weiser, 2002; 2004), remains controversial. Textural and geochemical arguments, such as the presence of inclusions of other PGM and Os isotope compositions, are considered by most researchers to reflect an origin of many of the Pt–Fe grains from high-temperature (i.e., magmatic) processes (e.g., Cabri et al., 1996; Weiser, 2002; Malitch and Thalhammer, 2002; Melcher et al., 2005; Okrugin, 2011).

In contrast, an opposing group has proposed a secondary origin of PGM in placers and soils (Augusthitis, 1965; Bowles, 1986; 1990; 1995; Ottemann and Augusthitis, 1967; Stumpfl, 1974; Cabral et al., 2007). Cousins (1973) and Cousins and Kinloch (1976) pointed out that size, shape, composition and microtexture of many eluvial and alluvial PGM differ from those observed in bedrocks and ores. They proposed formation of secondary PGM in a simplified process: (1) Serpentinization or weathering leads to the decomposition of base-metal sulfides carrying PGE in solid solution. (2) PGE are removed and transported as colloidal particles. (3) The colloids may coalesce or accrete to form larger particles and aggregates of PGE alloys. Textures such as zoning, reniform and mammillary textures are considered evidence for accretion and secondary growth in a low-temperature environment (Stumpfl, 1974; Cabral et al., 2007). Unconstrained three-dimensional growth, corrosion features on mineral faces, overplating of mineral faces, colloform and cyclic zonation, porous and spongy Pt-Fe nuggets, and overgrowths of one phase by another were considered unique to hydrothermal and supergene processes of formation (Bowles, 1995).

Cabri and Harris (1975) disputed a supergene origin of PGM as proposed by Augusthitis (1965). Cabri et al. (1996) and Weiser (2002 2004) cited only two likely exceptions where Pt nuggets may have formed in a surficial environment, namely palladian gold, potarite and native platinum in alluvial sediments from Devon, England, and botryoidal, zoned Pt–Pd nuggets from the

Bom Sucesso stream in Brazil. The Brazilian example has been critically evaluated by Fleet et al. (2002), who concluded that the alluvial PGM most likely originated from detrital grains that crystallized from low-temperature hydrothermal fluids. In their study of gold and PGM (isoferroplatinum and Os–Ir alloy) in offshore placers near Goodnews Bay, Alaska, Mardock and Barker (1991) found textures related to both derivation of PGM grains from mechanically weathered primary ore (i.e., typical assemblages of inclusions and exsolution phenomena) and subsequent accretion (i.e., microcrystalline assemblages of PGM in grain-rim cavities, suggesting leaching and crystallization). This important observation pertains to many occurrences of placer PGM; therefore, a combination of primary and secondary processes has to be considered to explain textural and chemical attributes of PGM nuggets.

Accordingly, possible sources of the Pt-Fe alloy grains comprise:

i. They are direct descendants from primary ores (Merensky Reef, UG-2, Platreef). This is improbable for all of them as they are generally present in subordinate proportions in pristine and oxidized ores, and a prolonged concentration and upgrading of these grains in the fluvial environment appears unlikely.
ii. The Pt-Fe alloy grains originate from disseminated occurrences in other rock units of the Bushveld Complex, e.g. chromitites. This possibility is not supported by the present work as possible contributions of Pt-Fe alloy grains from chromitites appear minimal.
iii. Pt-Fe alloy grains represent neo-formations that came into existence in the course of weathering of the Merensky Reef, UG-2, and Platreef ores and the concomitant supergene redistribution of the ore elements. Observations in the river sediments (presence of porous Pt and Pt-Fe alloy grains) and of PGM in ferralitic soils of Madagascar (Salpéteur et al., 1995) are in support of this hypothesis, but do not fully explain the quantity of Pt-Fe alloys present. Furthermore, some Pt-Fe alloy grains host a variety of inclusions of other PGM indicating a consanguineous, magmatic origin.

At the current state of knowledge, it must be speculated that some of the Pt-Fe alloy grains originate directly from the primary, pristine ores and others are true neo-formations that formed in the course of weathering of pristine ores and concomitant supergene redistribution of the PGE. Their precursor phases are either pre-existing, unstable PGM (note Pt coatings and partial replacements of cooperite/braggite and also of sperrylite), or they may even have formed via a solution stage under low-temperature conditions.

The assemblage of detrital PGM in alluvial sediments of rivers draining the Bushveld Complex largely mimics that of the Great Dyke in Zimbabwe (Oberthür et al., 2013a), where Pt and Pt-Fe alloys (42% by number of grains) are most common, followed by sperrylite (46%), cooperite/braggite (7%), and stibiopalladinite (1%). Apparently, the detrital PGM assemblages in rivers draining PGE-bearing layered intrusions (Bushveld, Great Dyke) display far-reaching similarities pointing to analogous starting materials (primary sulfide-bearing ores), processes of weathering, transport and deposition. Notably, these detrital PGM assemblages distinctly contrast to those derived from ophiolitic, generally uneconomic PGE mineralization (Cabri et al., 1996; Weiser, 2002; 2004) and therefore, can be regarded to represent useful indicators of platinum mineralization.

The concentrations of detrital PGM found in the various rivers are far from economic. In our earlier studies on the Maandagshoek placers (Oberthür et al., 2004; Melcher et al., 2005), up to some hundred grains of PGM were found in individual samples, corroborating the first findings of Merensky in 1924 (Wagner, 1929; Cawthorn, 1999). Furthermore, a large suite of about 30 different PGM was encountered, often being present in polyphase grains. This indicates that at Maandagshoek, a favourable combination of multiple, close-by sources (UG-2, Merensky Reef, Platinum Pipes) combined with special sedimentological circumstances are encountered. Probably, these comparatively rich accumulations represent residual material from the erosion of the thick terraces of unknown age still found on the sidewalls of the Moopetsi River.

The suite of eluvial PGM found on the eastern slope of the Onverwacht pipe basically represents the PGM assemblage described previously from the Onverwacht pipe proper by Genkin et al. (1966), Cabri et al. (1977a; b; c), Rudashevsky et al. (1992) and Zaccarini et al. (2002), including the Onverwacht pipe type locality minerals genkinite, irarsite and platarsite, as well as some additional and possibly new PGM. Furthermore, most of the relatively rare PGM detected in the suite of eluvial grains from Onverwacht largely resemble the alluvial PGM assemblage from Maandagshoek (Oberthür et al., 2004, Melcher et al., 2005), indicating that many of the alluvial grains do not originate from the Merensky or UG-2 reefs but from platiniferous pipes.

Finally, the detection of PGM in stream sediments by nowadays somewhat neglected simple field methods had their merits previously as detrital PGM acted as indicator minerals for platinum mineralization (e.g. Bushveld; Merensky, 1924; 1926; Cawthorn, 1999; Oberthür et al., 2004). The systematic recovery of PGM from stream sediments, soils and till should regain wider application in mineral exploration, especially when combined with PGM characterization by modern micro-analytical methods like hydroseparation and SEM work on concentrates (Oberthür et al., 2008; McClenagan and Cabri, 2011). It is emphasized that exploration work using basic techniques (sediment sampling, panning, microscopy) is far from outdated and can provide useful indicators to ore.

**Acknowledgements**

Thanks to Grant Cawthorn who ably guided us in the field and introduced us to the geology of the Bushveld. AngloPlatinum allowed access to their properties, which is gratefully acknowledged. Our BGR colleagues Lothar Gast, Christian Wöhrl and Ulrich Schwarz-Schampera were active panners and partners during our field work in 2000 and 2004 centering on the "Bushveld placers". Further sincere thanks go to Detlef Klosa who performed a great deal of the SEM work, and Jercy Lodziak patiently conducted the microprobe analyses. Hazel Prichard and Robert Schouwstra provided thorough reviews. Their valuable comments and suggestions are highly appreciated.

**References**

Augusthitis, S.S., 1965. Mineralogical and geochemical studies of the platiniferous dunite – birbirite – pyroxenite complex of Yubdo, Birbir, W. Ethiopia. Chemie der Erde, 24, 159-165.

Bowles, J.F.W., 1986. The development of platinum-group minerals in laterites. Economic Geology, 81, 1278-1285.

Bowles, J.F.W., 1990. Platinum-iron alloys, their structural and magnetic characteristics in relation to hydrothermal and low-temperature genesis. Mineralogy and Petrology, 43, 37-47.

Bowles, J.F.W., 1995. The development of platinum-group minerals (PGM) in laterites: mineral morphology. Chronique de la recherche minière, 520, 55-63.

Cabral, A.R., Beaudoin, G., Choquette, M., Lehmann, B. and Polônia, J.C., 2007. Supergene leaching and formation of platinum in alluvium: evidence from Serro, Minas Gerais, Brazil. Mineralogy and Petrology, 90, 141-150.

Cabri, L.J. (2002). The platinum-group minerals. In: L.J. Cabri (Editor), Canadian Institute of Mining, Metallurgy and Petroleum, CIM Special Volume, 54, 13-129.

Cabri, L.J., Feather, C.E. and Stewart, J.M., 1977b. Platinum-group minerals from Onverwacht. II. Platarsite, a new sulfarsenide of platinum. Canadian Mineralogist, 15, 385-388.

Cabri, L.J. and Harris, D.C., 1975. Zoning in Os-Ir alloys and the relation of the geological and tectonic environment of the source rocks to the bulk Pt:Pt + Ir + Os ratio for placers. Canadian Mineralogist, 13, 266-274.

Cabri, L.J., Harris, D.C. and Weiser, T.W., 1996. The mineralogy and distribution of Platinum Group Mineral (PGM) placer deposits of the world. Exploration and Mining Geology, 5, 73-167.

Cabri, L.J., Rosenzweig, A. and Pinch, W.W., 1977a. Platinum-group minerals from Onverwacht. I. Pt-Fe-Cu-Ni alloys. Canadian Mineralogist, 15, 380-384.

Cabri, L.J., Stewart, J.M., Laflamme, J.H.G. and Szymanski, J.T., 1977c. Platinum-group minerals from Onverwacht. III. Genkinite, $(Pt,Pd)_4Sb_3$, a new mineral. Canadian Mineralogist, 15, 389-392.

Cawthorn, R.G., 1999. The discovery of the platiniferous Merensky Reef in 1924. South African Journal of Geology, 102, 178-183.

Cawthorn, R.G. and Lee, C., 1998. 8th International Platinum Symposium, field excursion to the Bushveld Complex, Excursion Guide, The Geological Society of South Africa and The South African Institute of Mining and Metallurgy, 112pp.

Cawthorn, R.G., Lee, C.A., Schouwstra, R.P. and Mellowship, P., 2002. Relationship between PGE and PGM in the Bushveld Complex. Canadian Mineralogist, 40, 311-328.

Cousins, C.A., 1973. Platinoids of the Witwatersrand system. Journal of the South African Institute of Mining and Metallurgy, 73, 184-199.

Cousins, C.A. and Kinloch, E.D., 1976. Some observations on textures and inclusions in alluvial platinoids. Economic Geology, 71, 1377-1398.

Evans, D.M., Buchanan, D.L. and Hall, G.E.M., 1994. Dispersion of platinum, palladium and gold from the Main Sulphide Zone, Great Dyke, Zimbabwe. Transactions of the Institute of Mining and Metallurgy, 103, B57-B67.

Fleet, M.E., De Almeida, C.M. and Angeli, N., 2002. Botryoidal platinum, palladium and potarite from the Bom Sucesso stream, Minas Gerais, Brazil: compositional zoning and origin. Canadian Mineralogist, 40, 341-355.

Genkin, A.D., Zhuravlev, N.N., Troneva, N.V. and Murav'eva, I.V., 1966. Irarsite, a new sulfarsenide of iridium, rhodium, ruthenium, and platinum. Zapiski Vsesoyuznogo Mineralogicheskogo Obshchestva, 95, 700-712 (in Russian)

Harris, D. and Cabri, L.C., 1991. Nomenclature of platinum-group element alloys: Review and revision. Canadian Mineralogist, 29, 231-237.

Junge, M., Oberthür, T. and Melcher, F., 2014. Cryptic variation of chromite chemistry, platinum-group-element and -mineral distribution in the UG-2 chromitite – an example from the Karee Mine, western Bushveld Complex, South Africa. Economic Geology, 109, 795-810.

Kinloch, E.D., 1982. Regional trends in platinum-group mineralogy of the Critical Zone of the Bushveld Complex, South Africa. Economic Geology, 77, 1328-1347.

Malitch, K.N. and Thalhammer, O.A.R., 2002. Pt-Fe nuggets from clinopyroxenite-dunite massifs, Russia: a structural, compositional and osmium-isotope study. Canadian Mineralogist, 40, 395-417.

Mardock, C.L. and Barker, J.C., 1991. Theories on the transport and deposition of gold and PGM minerals in offshore placers near Goodnews Bay, Alaska. Ore Geology Reviews, 6, 211-227.

McClenagan, M.B. and Cabri, L.J., 2011. Review of gold and platinum group element (PGE) indicator minerals methods for surficial sediment sampling. Geochemistry: Exploration, Environment, Analysis, 11, 251-263.

Melcher, F. and Lodziak, J., 2007. Platinum-group minerals of concentrates from the Driekop platinum pipe, eastern Bushveld Complex – tribute to Eugen Stumpfl. Neues Jahrbuch für Mineralogie Abhandlungen, 183, 173-195.

Melcher, F., Oberthür, T. and Lodziak, J., 2005. Modification and alteration of detrital platinum-group minerals from the Eastern Bushveld Complex, South Africa. Canadian Mineralogist, 43, 1711-1734.

Merensky, H., 1924. The various platinum occurrences on the farm Maandagshoek No. 148. Unpublished memorandum to Lydenburg Platinum Syndicate. Archives of the Merensky Trust, Duivelskloof (Modjadjiskloof), South Africa.

Merensky, H., 1926. Die neuentdeckten Platinfelder im mittleren Transvaal und ihre wirtschaftliche Bedeutung. Zeitschrift Deutsche Geologische Gesellschaft, 78, 296-314.

Nickel, E.H., 1992. Solid solutions in mineral nomenclature. Canadian Mineralogist, 30, 231-234.

Oberthür, T., 2011. Platinum-Group Element Mineralization of the Main Sulfide Zone, Great Dyke, Zimbabwe. Reviews in Economic Geology, 17, 329–349.

Oberthür, T., Melcher, F., Buchholz, P. and Locmelis, M., 2013b. The oxidized ores of the Main Sulfide Zone, Great Dyke, Zimbabwe: Turning resources into minable reserves – mineralogy is the key. Journal of the Southern African Institute of Mining and Metallurgy, 133, 191-201.

Oberthür, T., Melcher, F., Gast, L., Wöhrl, Ch. and Lodziak, J., 2004. Detrital platinum-group minerals in rivers draining the eastern Bushveld Complex, South Africa. Canadian Mineralogist, 42, 563-582.

Oberthür, T., Melcher, F., Sitnikova, M., Rudashevsky, N.S., Rudashevsky, V.N., Cabri, L.J., Lodziak, J., Klosa, D. and Gast, L., 2008. Combination of Novel Mineralogical Methods in the Study of Noble Metal Ores – Focus on Pristine (Bushveld, Great Dyke) and Placer Platinum Mineralisation. Proceedings, 9th International Congress Applied Mineralogy (ICAM), Brisbane, Queensland, Australia, 187-194.

Oberthür, T., Weiser, T.W., Gast, L. and Kojonen, K., 2003 – Geochemistry and mineralogy of the platinum-group elements at Hartley Platinum Mine, Zimbabwe. Part 1: Primary distribution patterns in pristine ores of the Main Sulfide Zone of the Great Dyke. – Mineralium Deposita 38, 327-343. Part 2: Supergene redistribution in the oxidized Main Sulfide Zone of the Great Dyke, and alluvial platinum-group minerals. – Mineralium Deposita 38, 344-355.

Oberthür, T., Weiser, T.W., Melcher, F., Gast, L. and Wöhrl, C., 2013a. Detrital platinum-group minerals in rivers draining the Great Dyke, Zimbabwe. Canadian Mineralogist, 51, 197-222.

Okrugin, A.V., 2011. Origin of platinum-group minerals in mafic and ultramafic rocks: from dispersed elements to nuggets. Canadian Mineralogist, 49, 1397-1412.

Osbahr, I., Klemd, R., Oberthür, T., Brätz, H. and Schouwstra, R., 2013. Platinum-group element distribution in base-metal sulfides of the Merensky Reef from the eastern and western Bushveld Complex, South Africa. Mineralium Deposita, 48, 211-232.

Osbahr, I., Oberthür, T., Klemd, R., and Josties, A., 2014. Platinum-group element distribution in base-metal sulfides of the UG2, Bushveld Complex, South Africa – a reconnaissance study. Mineralium Deposita, 49, 655-665.

Ottemann, J. and Augusthitis, S.S., 1967. Geochemistry and origin of "platinum-nuggets" in laterite covers from ultrabasic rocks and birbirites of W. Ethiopia. Mineralium Deposita, 1, 269-277.

Pouchou, J.-L. and Pichoir, F., 1991. Quantitative analysis of homogeneous or stratified microvolumes applying the model "PAP" in microprobe analysis. In: K.F.J. Heinrich and D.E. Newbury (Editors). Electron Probe Quantitation. Plenum Press, New York, U.S.A., 31-75.

Rudashevsky, N.S., Avdontsev, S.N. and Dneprovskaya, M.B., 1992. Evolution of PGE mineralization in hortonolitic dunites of the Mooihoek and Onverwacht pipes, Bushveld Complex. Mineralogy and Petrology, 47, 37-54.

Salpeteur, I., Martin-Jantin, B. and Rakotomanana, D., 1995. Pt and Pd mobility in ferralitic soils of the West Andriamena area (Madagascar). Evidence of a supergene origin of some Pt and Pd minerals. Chronique de la recherche minière, 520, 27-45.

Schouwstra, R.P., Kinloch, E.D. and Lee C.A., 2000. A Short Geological Review of the Bushveld Complex. Platinum Metals Reviews, 44, 33-40.

Stumpfl, E.F., 1974. The genesis of platinum deposits: further thoughts. Minerals Science Engineering, 6, 120-141.

Stumpfl, E.F. and Clark, E., 1965. Hollingworthite, a new mineral. American Mineralogist, 50, 1068.

Tarkian, M. and Stumpfl, E.F., 1975. Platinum mineralogy of the Driekop mine, South Africa. Mineralium Deposita, 10, 71-85.

Wagner, P.A., 1929. The Platinum Deposits and Mines of South Africa. Oliver & Boyd, London, U.K., 326pp.

Weiser, T.W., 2002. Platinum-group minerals (PGM) in placer deposits. In: L.J. Cabri (Editor), Canadian Institute of Mining, Metallurgy and Petroleum, CIM Special Volume, 54, 721-756.

Weiser, T.W., 2004. Platinum-Group Minerals (PGM) from placer deposits in the mineral collection of the Museum of Natural History, Vienna, Austria. Annalen des Naturhistorischen Museums in Wien, 105A, 1-28.

Wilhelm, H.J., Zhang, H., Chen, F.L., Elsenbroek, J.H., Lombard, M. and de Bruin, D., 1997. Geochemical exploration for platinum-group elements in the Bushveld Complex, South Africa. Mineralium Deposita, 32, 349-361.

Zaccarini, F., Garuti, G. and Cawthorn, R.G., 2002. Platinum-group minerals in chromitite xenoliths from the Onverwacht and Tweefontein ultramafic pipes, eastern Bushveld Complex. Canadian Mineralogist, 40, 481-97.

Editorial handling: J.M. Barton Jr.